GEOLOGY | THE GEOLOGICAL SOCIETY OF AMERICA®

https://doi.org/10.1130/G46418.1

Manuscript received 25 April 2019
Revised manuscript received 20 July 2019
Manuscript accepted 6 August 2019

Published online 6 September 2019

Cenozoic carbonate burial along continental margins

Robin van der Ploeg[1]*, Bernard P. Boudreau[2], Jack J. Middelburg[1] and Appy Sluijs[1]
[1]Department of Earth Sciences, Faculty of Geosciences, Utrecht University, 3584 CB Utrecht, Netherlands
[2]Department of Oceanography, Dalhousie University, Halifax, Nova Scotia B3H4R2, Canada

ABSTRACT

Marine carbonate burial represents the largest long-term carbon sink at Earth's surface, occurring in both deep-sea (pelagic) environments and shallower waters along continental margins. The distribution of carbonate accumulation has varied over geological history and impacts the carbon cycle and ocean chemistry, but it remains difficult to quantitatively constrain. Here, we reconstruct Cenozoic carbonate burial along continental margins using a mass balance for global carbonate alkalinity, which integrates independent estimates for continental weathering and pelagic carbonate burial. Our results indicate that major changes in marginal carbonate burial were associated with important climate and sea-level change events, including the Eocene-Oligocene transition (ca. 34 Ma), the Oligocene-Miocene boundary Mi-1 glaciation (ca. 23 Ma), and the middle Miocene climate transition (ca. 14 Ma). In addition, we find that a major increase in continental weathering from ca. 10 Ma to the present may have driven a concomitant increase in pelagic carbonate burial. Together, our results show that changes in global climate, sea level, and continental weathering have all impacted carbonate burial over the Cenozoic, but the relative importance of these processes may have varied through time.

INTRODUCTION

Marine calcium carbonate ($CaCO_3$) deposition occurs on continental shelves and slopes, and in the open ocean above the carbonate compensation depth (CCD; Milliman, 1993). At present, deep-sea (hereafter termed pelagic) carbonate burial represents ~55%–65% of global carbonate burial, while carbonate accumulation along continental margins (including both shelves and slopes; hereafter termed marginal environments, or margins) accounts for the rest (Mackenzie and Morse, 1992). Carbonate alkalinity is delivered to the oceans mainly by silicate and carbonate rock weathering, and it is removed by carbonate burial, either in marginal or pelagic environments. These alkalinity inputs and outputs should be in balance over geological time scales (Berner, 2004; Ridgwell and Zeebe, 2005). This does not require true steady-state conditions, but it implies that input and output processes adjust sufficiently fast to changes to maintain balance at any given time on secular time scales (Boudreau et al., 2019). However, the nature and dominant location of carbonate accumulation have shifted over geological history, in association with changes in plate tectonics, paleogeography, global sea level, climate, ocean chemistry and the evolution of calcifying organisms (Mackenzie and Morse, 1992; Stanley and Hardie, 1998; Ridgwell and Zeebe, 2005). High sea levels resulted in extensive shallow-water carbonate accumulation in epicontinental seas during parts of the Phanerozoic, notably during the Carboniferous and Cambrian (Hay, 1985; Opdyke and Wilkinson, 1988; Walker et al., 2002), while pelagic carbonate burial was insignificant until the evolutionary success of coccolithophores and planktonic foraminifera in the Mesozoic (Martin, 1995; Ridgwell, 2005). An overall, long-term decline in marginal deposition since the Late Cretaceous in response to falling sea levels and a reduction in epicontinental shelf areas may have resulted in a further increase in pelagic deposition toward the present (Opdyke and Wilkinson, 1988; Walker et al., 2002).

For carbon cycle reconstructions, it is important to resolve temporal changes in marginal and pelagic carbonate burial and their respective contributions to global carbonate accumulation. Because the continental margins represent the transition zone between the terrestrial and marine realms, they may either act as a carbon sink through immediate carbonate burial, or as a carbon source to the pelagic oceans through carbonate export. Additionally, marginal carbonates are deposited as aragonite, calcite, and magnesium-rich calcite, whereas pelagic carbonates are deposited primarily as calcite (Milliman, 1993). Because of these differences in carbonate mineralogy, shifts in marginal and pelagic carbonate burial may also drive changes in ocean chemistry (Berner, 2004). Progress has been made to estimate pelagic carbonate burial rates through time (Opdyke and Wilkinson, 1988; Boudreau and Luo, 2017), but relatively little is still known about secular changes in marginal carbonate burial. Here, we employ a new approach to estimate marginal carbonate burial rates for the Cenozoic, based on a mass balance for global carbonate alkalinity that incorporates independent continental weathering and pelagic carbonate burial histories.

METHODS

We derive a steady-state carbonate alkalinity mass balance for the present, where alkalinity is delivered to the oceans by continental weathering ($F_{weathering}$) and anaerobic processes in organic-rich sediments deposited along continental margins ($F_{anaerobic}$), while alkalinity is removed through marginal and pelagic carbonate burial ($F_{margins}$ and $F_{pelagic}$, respectively; Fig. DR1 in the GSA Data Repository[1]). We calculate changes in $F_{weathering}$ for the Cenozoic based on inverse modeling of the marine strontium (Sr) and osmium (Os) isotope systems, two well-established tracers for weathering inputs to the global ocean (Ravizza and Zachos, 2003; see also the Data Repository). We use published

*E-mail: R.vanderPloeg@uu.nl

[1]GSA Data Repository item 2019362, supplementary information including detailed model descriptions and sensitivity analyses, is available online at http://www.geosociety.org/datarepository/2019/, or on request from editing@geosociety.org.

CITATION: van der Ploeg, R., et al., 2019, Cenozoic carbonate burial along continental margins: Geology, v. 47, p. 1025–1028, https://doi.org/10.1130/G46418.1

Cenozoic seawater $^{87}Sr/^{86}Sr$ records (McArthur et al., 2012) and $^{187}Os/^{188}Os$ records (Klemm et al., 2005; Burton, 2006; Nielsen et al., 2009) in combination with seafloor spreading and/or degassing rate reconstructions (e.g., Van Der Meer et al., 2014) to estimate changes in continental silicate weathering and sediment weathering—the sum of carbonate weathering and organic-rich sediment weathering—back in time (Figs. DR2–DR6 in the Data Repository). This approach is inspired by previous modeling studies (Delaney and Boyle, 1988; Li et al., 2009; Li and Elderfield, 2013) and uses the same Sr and Os isotope data sets as Li and Elderfield (2013), but, uniquely, we do not assume a priori equilibrium between inputs and outputs in our weathering reconstructions. Rather, we consider the Sr and Os isotope systems without incorporating additional mass balance constraints (e.g., carbon isotopes), which enabled us to independently use the carbonate alkalinity mass balance to subsequently derive marginal carbonate burial. We investigate a range of scenarios for continental silicate weathering and sediment weathering based on different sets of assumptions regarding the evolution of their respective $^{87}Sr/^{86}Sr$ and $^{187}Os/^{188}Os$ compositions over the Cenozoic (either as constant values or as linear increases in one or multiple parameters; Table DR2; Fig. DR6). These continental silicate and sediment weathering estimates are proportionally added to obtain the total carbonate alkalinity delivery associated with continental weathering.

For $F_{anaerobic}$, we use the sum of alkalinity addition from net denitrification and pyrite burial, as estimated for the present-day by Hu and Cai (2011). Inverse modeling of carbon and sulfur isotope records has demonstrated that pyrite burial rates were likely higher in the early Cenozoic than at present (Rennie et al., 2018), but the resulting changes in alkalinity fluxes are rather small compared to those associated with continental weathering and carbonate burial. Therefore, we choose to maintain a constant value of $F_{anaerobic}$ over the Cenozoic within the uncertainties reported by Hu and Cai (2011).

Boudreau and Luo (2017) estimated Cenozoic changes in $F_{pelagic}$ independent of any continental weathering reconstructions. These estimates were derived using a set of equations that related pelagic carbonate burial rates to the positions of the calcite saturation horizon and the CCD. Based on this work, we derive two different scenarios for $F_{pelagic}$, driven by either the global Cenozoic CCD curve (Lyle et al., 2008; i.e., the Delaney and Boyle [1988] compilation with an updated age model) or the Pacific CCD curve for the past 50 m.y. (Fig. 1F; Pälike et al., 2012). The Lyle et al. (2008) CCD includes information from all major ocean basins and thus represents global trends, although coverage of Atlantic Ocean sites is relatively poor. The Pacific CCD record of Pälike et al. (2012) is only an approximation of global CCD change, but this record is still useful because the Pacific Ocean represents the largest ocean basin by volume—even more so in the early Cenozoic than at present (Lyle et al., 2008). However, the CCD may have been relatively insensitive to changes in weathering and carbonate burial during the early Eocene (Greene et al., 2019).

Finally, Cenozoic changes in $F_{margins}$ are calculated by solving our carbonate alkalinity mass balance through time, with propagation of uncertainties in $F_{weathering}$, $F_{anaerobic}$, and $F_{pelagic}$ (see the Data Repository).

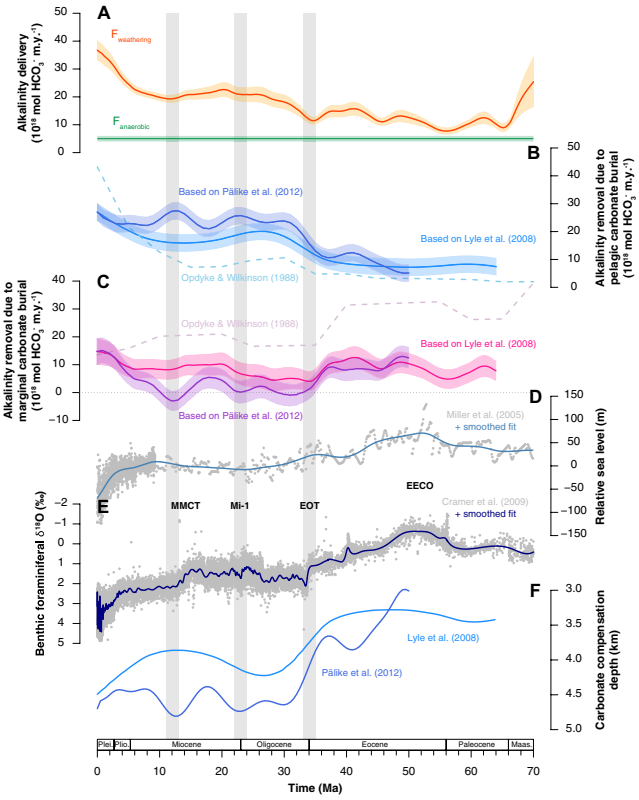

Figure 1. Modeled alkalinity delivery and removal rates for the Cenozoic in relation to global climate and sea level. (A) Alkalinity delivery from continental weathering, $F_{weathering}$ (red), inferred from Sr and Os cycle modeling. Orange-shaded areas represent minimum and maximum estimates based on the full range of scenarios presented in the Data Repository (see footnote 1), and the solid red line represents the mean of these estimates. Alkalinity delivery from anaerobic processes along continental margins, $F_{anaerobic}$ (green), kept constant over the Cenozoic within the range of present-day estimates by Hu and Cai (2011). (B) Alkalinity removal due to pelagic carbonate burial, $F_{pelagic}$, based on estimates of Boudreau and Luo (2017), following either Lyle et al.'s (2008) carbonate compensation depth (CCD; light blue) or Pälike et al.'s (2012) CCD (dark blue). Shaded areas represent minimum and maximum estimates based on present-day estimates of either Davies and Worsley (1981) or Mackenzie and Morse (1992). Dashed blue line represents pelagic carbonate burial rates as reconstructed by Opdyke and Wilkinson (1988) and adjusted to alkalinity equivalents. (C) Alkalinity removal due to marginal carbonate burial, $F_{margins}$, calculated as the difference between $F_{weathering}$, $F_{anaerobic}$, and $F_{pelagic}$, following either Lyle et al.'s (2008) CCD (pink) or Pälike et al.'s (2012) CCD (purple) (see the Data Repository [see footnote 1]). Dashed purple line represents marginal carbonate burial rates as reconstructed by Opdyke and Wilkinson (1988), taken as the sum of their estimates for carbonate platform and slope-rise systems and adjusted to alkalinity equivalents. (D) Global sea-level curve of Miller et al. (2005), and (E) benthic foraminiferal $\delta^{18}O$ compilation of Cramer et al. (2009), both shown as individual data points (in gray) and as smoothed fits (in blue). (F) Smoothed fits to CCD records of Lyle et al. (2008) (light blue) and Pälike et al. (2012) (dark blue), as obtained from Boudreau and Luo (2017). EECO—early Eocene climatic optimum; EOT—Eocene-Oligocene transition, Mi-1—Mi-1 glaciation, and MMCT—middle Miocene climate transition.

RESULTS

Our range of $F_{weathering}$ scenarios displays a gradual increase from the early Cenozoic toward the present (Fig. 1A), a result consistent with previous modeling studies in terms of general shape and magnitude (Delaney and Boyle, 1988; Li and Elderfield, 2013). The large increase in $F_{weathering}$ we predict in the late Neogene coincides roughly with the final stage of Himalayan uplift (Raymo et al., 1988), but the impact of Himalayan uplift on continental weathering rates remains in debate because weathering reconstructions are generally nonunique and different weathering proxies offer contrasting views (Kump, 1989; Edmond, 1992; Lear et al., 2003; Willenbring and Von Blanckenburg, 2010; Caves Rugenstein et al., 2019). By comparison, the contribution of $F_{anaerobic}$ to alkalinity delivery is small for most of the Cenozoic.

The $F_{pelagic}$ scenarios show an overall increase toward the present, but they diverge during the Oligocene and especially during the Miocene (Fig. 1B). This divergence is due to underlying differences between the Lyle et al. (2008) CCD and the Pälike et al. (2012) CCD. In particular, the latter may contain departures from global trends because it also responds to changes in equatorial Pacific carbonate production relative to global carbonate production, or changes in carbonate deposition fractionation between the

Atlantic and Pacific basins. The general shape of the Lyle et al. (2008)–based $F_{pelagic}$ scenario appears to correspond best to the reconstructions of pelagic carbonate accumulation of Opdyke and Wilkinson (1988).

If our independent $F_{weathering}$, $F_{anaerobic}$, and $F_{pelagic}$ estimates are robust, secular trends in $F_{margins}$ should emerge that fit existing observations from the geological record (Fig. 1C). The Lyle et al. (2008)–based $F_{margins}$ scenario is relatively smooth for most of the Cenozoic, except for one interval of rapid change. After a gradual increase in the Eocene, $F_{margins}$ displays a major decrease between 38 and 34 Ma, followed by an interval where the rates become quite low. These low values persist during most of the Oligocene until ca. 23 Ma, after which $F_{margins}$ recovers and remains constant until the end of the Miocene. A small, final increase is observed between the Pliocene and the present. The Pälike et al. (2012)–based $F_{margins}$ scenario displays more dramatic shifts than the Lyle et al. (2008)–based scenario, but it does not extend beyond 50 Ma. Following a slight decline in the Eocene, it is characterized by an interval of very low values between 36 and 10 Ma. This interval is punctuated by distinct minima with negative burial rates at ca. 32 Ma, ca. 23 Ma, and ca. 12 Ma, which indicate net removal (weathering) of previously buried marginal carbonates and transport of alkalinity to the pelagic realm. Finally, a large increase is observed from ca. 10 Ma to the present that is not apparent in the Lyle et al. (2008)–based scenario.

DISCUSSION

We find that the overall patterns in $F_{margins}$ correlate with the Cenozoic evolution of global sea level and climate (Figs. 1D and 1E). For the early Cenozoic, we estimate relatively high $F_{margins}$ values corresponding to globally warm climates (Zachos et al., 2008) and high sea levels (Miller et al., 2005), while subsequent long-term cooling is generally mirrored by a decline in $F_{margins}$ values. The absolute $F_{margins}$ values we obtain are mostly lower than those reconstructed by Opdyke and Wilkinson (1988), potentially due to underestimation of $F_{weathering}$, $F_{anaerobic}$, or both in the early Cenozoic. Importantly, however, the distinct minima in $F_{margins}$ correlate with important episodes of sea-level change and loss of marginal environments. For example, the large $F_{margins}$ shift at ca. 36 Ma occurs just prior to the Eocene-Oligocene transition (ca. 34 Ma) and the onset of Antarctic glaciation (Lear et al., 2000), which was characterized by an episode of major sea-level fall and CCD deepening due to transient weathering of exposed shelf carbonates and a shift of carbonate burial to the pelagic oceans (Coxall et al., 2005; Merico et al., 2008; Armstrong McKay et al., 2016). Similarly, the minimum at ca. 23 Ma is virtually synchronous with ice-sheet expansion during the Oligocene-Miocene boundary Mi-1 glaciation (Miller et al., 1991; Zachos et al., 2001), and the minimum at ca. 12 Ma, which is only apparent in the Pälike et al. (2012)–based scenario, follows ice-sheet expansion just after the middle Miocene climate transition (ca. 14 Ma; Flower and Kennett, 1994; Shevenell et al., 2004; Armstrong McKay et al., 2014). The strong correlations between episodes of decreasing or negative $F_{margins}$ and major episodes of cooling and ice-sheet expansion suggest that these phenomena were related through changes in global sea level and carbonate compensation.

Strikingly, the Pälike et al. (2012)–based $F_{margins}$ scenario deviates from these aforementioned long-term Cenozoic trends over the past 10 m.y. The final $F_{margins}$ increase in this scenario results from a relatively invariant $F_{pelagic}$ at a time of strongly increasing $F_{weathering}$. However, this $F_{margins}$ increase would be opposite to the continued decrease in platform carbonate burial that has been inferred over this period by other studies (Hay, 1985; Opdyke and Wilkinson, 1988; Walker et al., 2002) and that would be expected based on progressive Cenozoic sea-level fall (Haq et al., 1987; Miller et al., 2005; Müller et al., 2008). By comparison, the Lyle et al. (2008)–based $F_{margins}$ scenario resembles the reconstructions of Opdyke and Wilkinson (1988) better over this period because the large $F_{weathering}$ increase is mostly accommodated by a simultaneous increase in $F_{pelagic}$. This reveals the potential of continental weathering as a driver of changes in pelagic carbonate burial, but this relationship may be variable through time due to changes in background climate states (e.g., Greene et al., 2019). Therefore, we suggest that future studies should focus on fully incorporating the complex interactions among climate, sea level, weathering, carbonate burial, and the CCD in models.

CONCLUSIONS

We present estimates of carbonate burial along continental margins for the Cenozoic, using a global alkalinity mass balance that incorporates independent estimates of continental weathering and pelagic carbonate burial. The correlation between the inferred changes in $F_{margins}$, $F_{pelagic}$, and the interplay of global climate, sea level, and continental weathering implies that these phenomena and processes have all impacted carbonate burial over the Cenozoic, but that their relative importance may have changed over time. In summary, global cooling and sea-level fall may have driven the progressive, long-term decline in marginal carbonate burial for most of the Cenozoic, while an increase in continental weathering related to tectonic uplift in the late Neogene may have driven the final pelagic carbonate burial increase toward the present. Additionally, these long-term trends appear to be modulated by transient climate events such as the Eocene-Oligocene transition, Mi-1 glaciation, and middle Miocene climate transition. Episodes of negative marginal carbonate burial associated with such climate events may indicate large-scale weathering and erosion of previously deposited carbonate material and release of alkalinity from the continental margins to the pelagic oceans, which is consistent with the concept of shifting carbonate accumulation through time.

ACKNOWLEDGMENTS

This work was carried out under the program of the Netherlands Earth System Science Centre (NESSC), which is financially supported by the Ministry of Education, Culture and Science (OCW) of the Netherlands. We thank Mitchell Lyle, Bradley Opdyke, Gerald Dickens, and David Armstrong McKay for constructive reviews that significantly improved the quality of this manuscript.

REFERENCES CITED

Armstrong McKay, D.I., Tyrrell, T., Wilson, P.A., and Foster, G.L., 2014, Estimating the impact of the cryptic degassing of large igneous provinces: A mid-Miocene case-study: Earth and Planetary Science Letters, v. 403, p. 254–262, https://doi.org/10.1016/j.epsl.2014.06.040.

Armstrong McKay, D.I., Tyrrell, T., and Wilson, P.A., 2016, Global carbon cycle perturbation across the Eocene-Oligocene climate transition: Paleoceanography, v. 31, p. 311–329, https://doi.org/10.1002/2015PA002818.

Berner, R.A., 2004, The Phanerozoic Carbon Cycle: CO_2 and O_2: Oxford, UK, Oxford University Press, 150 p.

Boudreau, B.P., and Luo, Y., 2017, Retrodiction of secular variations in deep-sea $CaCO_3$ burial during the Cenozoic: Earth and Planetary Science Letters, v. 474, p. 1–12, https://doi.org/10.1016/j.epsl.2017.06.005.

Boudreau, B.P., Middelburg, J.J., Sluijs, A., and van der Ploeg, R., 2019, Secular variations in the carbonate chemistry of the oceans over the Cenozoic: Earth and Planetary Science Letters, v. 512, p. 194–206, https://doi.org/10.1016/j.epsl.2019.02.004.

Burton, K.W., 2006, Global weathering variations inferred from marine radiogenic isotope records: Journal of Geochemical Exploration, v. 88, p. 262–265, https://doi.org/10.1016/j.gexplo.2005.08.052.

Caves Rugenstein, J.K., Ibarra, D.E., and von Blanckenburg, F., 2019, Neogene cooling driven by land surface reactivity rather than increased weathering fluxes: Nature, v. 571, p. 99–102, https://doi.org/10.1038/s41586-019-1332-y.

Coxall, H.K., Wilson, P.A., Pälike, H., Lear, C.H., and Backman, J., 2005, Rapid stepwise onset of Antarctic glaciation and deeper calcite compensation in the Pacific Ocean: Nature, v. 433, p. 53–57, https://doi.org/10.1038/nature03135.

Cramer, B.S., Toggweiler, J.R., Wright, J.D., Katz, M.E., and Miller, K.G., 2009, Ocean overturning since the Late Cretaceous: Inferences from a new benthic foraminiferal isotope compilation: Paleoceanography, v. 24, PA4216, https://doi.org/10.1029/2008PA001683.

Davies, T.A., and Worsley, T.R., 1981, Paleoenvironmental implications of oceanic carbonate sedimentation rates, *in* Warme, J.E., et al., eds., The Deep Sea Drilling Project: A Decade of Progress: Society of Economic Paleontologists and Mineralogists

(SEPM) Special Publications, v. 32, p. 169–179, https://doi.org/10.2110/pec.81.32.0169.
Delaney, M.L., and Boyle, E.A., 1988, Tertiary paleoceanic chemical variability: Unintended consequences of simple geochemical models: Paleoceanography, v. 3, p. 137–156, https://doi.org/10.1029/PA003i002p00137.
Edmond, J.M., 1992, Himalayan tectonics, weathering processes, and the strontium isotope record in marine limestones: Science, v. 258, p. 1594–1597, https://doi.org/10.1126/science.258.5088.1594.
Flower, B.P., and Kennett, J.P., 1994, The middle Miocene climatic transition: East Antarctic ice sheet development, deep ocean circulation and global carbon cycling: Palaeogeography, Palaeoclimatology, Palaeoecology, v. 108, p. 537–555, https://doi.org/10.1016/0031-0182(94)90251-8.
Greene, S.E., Ridgwell, A., Turner, S.K., Schmidt, D.N., Pälike, H., Thomas, E., Greene, L.K., and Hoogakker, B.A.A., 2019, Early Cenozoic decoupling of climate and carbonate compensation depth trends: Paleoceanography and Paleoclimatology, v. 34, no. 6, p. 930–945, https://doi.org/10.1029/2019pa003601.
Haq, B.U., Hardenbol, J., and Vail, P.R., 1987, Chronology of fluctuating sea levels since the Triassic: Science, v. 235, p. 1156–1167, https://doi.org/10.1126/science.235.4793.1156.
Hay, W.W., 1985, Potential errors in estimates of carbonate rock accumulating through geologic time, *in* Sundquist, E.T., and Broecker, W.S., eds., The Carbon Cycle and Atmospheric CO_2: Natural Variations Archean to Present: American Geophysical Union Geophysical Monograph 32, p. 573–583, https://doi.org/10.1029/GM032p0573.
Hu, X., and Cai, W.J., 2011, An assessment of ocean margin anaerobic processes on oceanic alkalinity budget: Global Biogeochemical Cycles, v. 25, GB3003, https://doi.org/10.1029/2010GB003859.
Klemm, V., Levasseur, S., Frank, M., Hein, J.R., and Halliday, A.N., 2005, Osmium isotope stratigraphy of a marine ferromanganese crust: Earth and Planetary Science Letters, v. 238, p. 42–48, https://doi.org/10.1016/j.epsl.2005.07.016.
Kump, L.R., 1989, Alternative modeling approaches to the geochemical cycles of carbon, sulfur, and strontium isotopes: American Journal of Science, v. 289, p. 390–410, https://doi.org/10.2475/ajs.289.4.390.
Lear, C.H., Elderfield, H., and Wilson, P.A., 2000, Cenozoic deep-sea temperatures and global ice volumes from Mg/Ca in benthic foraminiferal calcite: Science, v. 287, p. 269–272, https://doi.org/10.1126/science.287.5451.269.
Lear, C.H., Elderfield, H., and Wilson, P.A., 2003, A Cenozoic seawater Sr/Ca record from benthic foraminiferal calcite and its application in determining global weathering fluxes: Earth and Planetary Science Letters, v. 208, p. 69–84, https://doi.org/10.1016/S0012-821X(02)01156-1.
Li, G., and Elderfield, H., 2013, Evolution of carbon cycle over the past 100 million years: Geochimica et Cosmochimica Acta, v. 103, p. 11–25, https://doi.org/10.1016/j.gca.2012.10.014.
Li, G., Ji, J., Chen, J., and Kemp, D.B., 2009, Evolution of the Cenozoic carbon cycle: The roles of tectonics and CO_2 fertilization: Global Biogeochemical Cycles, v. 23, GB1009, https://doi.org/10.1029/2008GB003220.
Lyle, M., Barron, J., Bralower, T.J., Huber, M., Lyle, A.O., Ravelo, A.C., Rea, D.K., and Wilson, P.A., 2008, Pacific Ocean and Cenozoic evolution of climate: Reviews of Geophysics, v. 46, p. 1–47, https://doi.org/10.1029/2005RG000190.
Mackenzie, F.T., and Morse, J.W., 1992, Sedimentary carbonates through Phanerozoic time: Geochimica et Cosmochimica Acta, v. 56, p. 3281–3295, https://doi.org/10.1016/0016-7037(92)90305-3.
Martin, R.E., 1995, Cyclic and secular variation in microfossil biomineralization: Clues to the biogeochemical evolution of Phanerozoic oceans: Global and Planetary Change, v. 11, p. 1–23, https://doi.org/10.1016/0921-8181(94)00011-2.
McArthur, J.M., Howarth, R.J., and Shields, G.A., 2012, Strontium isotope stratigraphy, *in* Gradstein, F.M., Ogg, J.G., Schmitz, M., and Ogg, G., eds., The Geologic Time Scale, Volume 1: Amsterdam, Netherlands, Elsevier, p. 127–144, https://doi.org/10.1016/B978-0-444-59425-9.00007-X.
Merico, A., Tyrrell, T., and Wilson, P.A., 2008, Eocene/Oligocene ocean de-acidification linked to Antarctic glaciation by sea-level fall: Nature, v. 452, p. 979–982, https://doi.org/10.1038/nature06853.
Miller, K.G., Wright, J.D., and Fairbanks, R.G., 1991, Unlocking the ice house: Oligocene–Miocene oxygen isotopes, eustasy, and margin erosion: Journal of Geophysical Research–Solid Earth, v. 96, p. 6829–6848, https://doi.org/10.1029/90JB02015.
Miller, K.G., Kominz, M.A., Browning, J.V., Wright, J.D., Mountain, G.S., Katz, M.E., Sugarman, P.J., Cramer, B.S., Christie-Blick, N., and Pekar, S.F., 2005, The Phanerozoic record of global sea-level change: Science, v. 310, p. 1293–1298, https://doi.org/10.1126/science.1116412.
Milliman, J.D., 1993, Production and accumulation of calcium carbonate in the ocean: Budget of a nonsteady state: Global Biogeochemical Cycles, v. 7, p. 927–957, https://doi.org/10.1029/93GB02524.
Müller, R.D., Sdrolias, M., Gaina, C., Steinberger, B., and Heine, C., 2008, Long-term sea-level fluctuations driven by ocean basin dynamics: Science, v. 319, p. 1357–1362, https://doi.org/10.1126/science.1151540.
Nielsen, S.G., Mar-Gerrison, S., Gannoun, A., LaRowe, D., Klemm, V., Halliday, A.N., Burton, K.W., and Hein, J.R., 2009, Thallium isotope evidence for a permanent increase in marine organic carbon export in the early Eocene: Earth and Planetary Science Letters, v. 278, p. 297–307, https://doi.org/10.1016/j.epsl.2008.12.010.
Opdyke, B.N., and Wilkinson, B.H., 1988, Surface area control of shallow cratonic to deep marine carbonate accumulation: Paleoceanography, v. 3, p. 685–703, https://doi.org/10.1029/PA003i006p00685.
Pälike, H., et al., 2012, A Cenozoic record of the equatorial Pacific carbonate compensation depth: Nature, v. 488, p. 609–614, https://doi.org/10.1038/nature11360.
Ravizza, G.E., and Zachos, J.C., 2003, Records of Cenozoic ocean chemistry, *in* Holland, H.D., and Turekian, K.K., eds., Treatise on Geochemistry, Volume 6: Amsterdam, Netherlands, Elsevier, p. 551–581, https://doi.org/10.1016/B0-08-043751-6/06121-1.
Raymo, M.E., Ruddiman, W.F., and Froelich, P.N., 1988, Influence of late Cenozoic mountain building on ocean geochemical cycles: Geology, v. 16, p. 649–653, https://doi.org/10.1130/0091-7613(1988)016<0649.
Rennie, V.C.F., Paris, G., Sessions, A.L., Abramovich, S., Turchyn, A.V., and Adkins, J.F., 2018, Cenozoic record of $\delta^{34}S$ in foraminiferal calcite implies an early Eocene shift to deep-ocean sulfide burial: Nature Geoscience, v. 11, p. 761–765, https://doi.org/10.1038/s41561-018-0200-y.
Ridgwell, A., 2005, A mid-Mesozoic revolution in the regulation of ocean chemistry: Marine Geology, v. 217, p. 339–357, https://doi.org/10.1016/j.margeo.2004.10.036.
Ridgwell, A., and Zeebe, R.E., 2005, The role of the global carbonate cycle in the regulation and evolution of the Earth system: Earth and Planetary Science Letters, v. 234, p. 299–315, https://doi.org/10.1016/j.epsl.2005.03.006.
Shevenell, A.E., Kennett, J.P., and Lea, D.D., 2004, Middle Miocene Southern Ocean cooling and Antarctic cryosphere expansion: Science, v. 305, p. 1766–1770, https://doi.org/10.1126/science.1100061.
Stanley, S.M., and Hardie, L.A., 1998, Secular oscillations in the carbonate mineralogy of reef-building and sediment-producing organisms driven by tectonically forced shifts in seawater chemistry: Palaeogeography, Palaeoclimatology, Palaeoecology, v. 144, p. 3–19, https://doi.org/10.1016/S0031-0182(98)00109-6.
Van Der Meer, D.G., Zeebe, R.E., van Hinsbergen, D.J.J., Sluijs, A., Spakman, W., and Torsvik, T.H., 2014, Plate tectonic controls on atmospheric CO_2 levels since the Triassic: Proceedings of the National Academy of Sciences of the United States of America, v. 111, p. 4380–4385, https://doi.org/10.1073/pnas.1315657111.
Walker, L.J., Wilkinson, B.H., and Ivany, L.C., 2002, Continental drift and Phanerozoic carbonate accumulation in shallow-shelf and deep-marine settings: The Journal of Geology, v. 110, p. 75–87, https://doi.org/10.1086/324318.
Willenbring, J.K., and Von Blanckenburg, F., 2010, Long-term stability of global erosion rates and weathering during late Cenozoic cooling: Nature, v. 465, p. 211–214, https://doi.org/10.1038/nature09044.
Zachos, J.C., Pagani, M., Sloan, L., Thomas, E., and Billups, K., 2001, Trends, rhythms, and aberrations in global climate 65 Ma to present: Science, v. 292, p. 686–693 https://doi.org/10.1126/science.1059412.
Zachos, J.C., Dickens, G.R., and Zeebe, R.E., 2008, An early Cenozoic perspective on greenhouse warming and carbon-cycle dynamics: Nature, v. 451, p. 279–283, https://doi.org/10.1038/nature06588.

Printed in USA